JOURNAL OF THE ROYAL SOCIETY Interface

rsif.royalsocietypublishing.org

Research

Cite this article: Nicasio-Collazo LA, Delgado-González A, Castañeda-Priego R, Hernández-Lemus E. 2014 Stress-induced DNA damage: a case study in diffuse large B-cell lymphoma. *J. R. Soc. Interface* **11**: 20140785.
http://dx.doi.org/10.1098/rsif.2014.0785

Received: 18 July 2014
Accepted: 18 August 2014

Subject Areas:
biophysics, systems biology, chemical physics

Keywords:
DNA denaturation, B-cell lymphoma, non-equilibrium thermodynamics

Authors for correspondence:
Ramón Castañeda-Priego
e-mail: ramoncp@fisica.ugto.mx
Enrique Hernández-Lemus
e-mail: ehernandez@inmegen.gob.mx

Electronic supplementary material is available at http://dx.doi.org/10.1098/rsif.2014.0785 or via http://rsif.royalsocietypublishing.org.

Royal Society Publishing

Stress-induced DNA damage: a case study in diffuse large B-cell lymphoma

Luz Adriana Nicasio-Collazo[1], Alexandra Delgado-González[1], Ramón Castañeda-Priego[1] and Enrique Hernández-Lemus[2,3]

[1]Division of Sciences and Engineering, University of Guanajuato, León, Mexico
[2]Department of Computational Genomics, National Institute of Genomic Medicine, Mexico City, Mexico
[3]Complexity in Systems Biology, Center for Complexity Sciences, National Autonomous University of México, Mexico City, Mexico

DNA damage is one of the mechanisms of mutagenesis. Sequence integrity may be affected by the action of thermal changes, chemical agents, both endogenous and exogenous, and other environmental issues. Abnormally high mutation rates are referred to as *genomic instability*: a phenomenon closely related to the onset of cancer. Mutant genotypes may be able to confer some kind of selective advantage on subclonal cell populations, leading them to multiply until dominance in a localized tissue environment that later becomes the tumour. Cellular stress, especially that of oxidative and ionic nature, is a recognized trigger for DNA-damaging processes. A physico-chemical model has shown that high hysteresis rates in DNA denaturation curves may be indicative of dissipative processes inducing DNA damage, thus potentially leading to uncontrolled mutagenesis and genome instability. We here study selectively to what extent this phenomenon may occur by analysing the sequence length and composition effects on the thermodynamic behaviour and the presence of hysteresis in pressure-driven DNA denaturation; pronounced hysteresis in the denaturation/renaturation curves may indicate thermal susceptibility to DNA damage. In particular, we consider highly mutated regions of the genome characterized in diffuse large B-cell lymphoma on a recent whole exome next-generation sequencing effort.

1. Introduction

Biophysical approaches are becoming increasingly valuable to understand cancer biology. One important example may be found in the study of *DNA damage*; the molecular degradation of genomic information due to physico-chemical variations in the DNA molecule. Such variations (mutations) may be produced by a variety of endogenous and exogenous mechanisms [1,2]. By understanding the biophysical mechanisms underlying DNA damage and its associated biochemical consequences, molecular biologists and oncologists may be better equipped to attack the foundations of *genome instability* that, according to our current understanding, may be behind the ultimate origins of cancer.

In this work, we make use of our recent molecular model for the thermodynamical response of DNA to both ionic stress and temperature variations [3], and we study the thermodynamic effects of ionic stress in some genes that have significant mutation rates, essential for the pathogenesis of diffuse large B-cell lymphoma (DLBCL) [4]. This systematic study allows us to present, for the first time, a *hysteresis map* that may be associated with stress-induced DNA damage in DLBCL.

The DNA molecule, the ultimate repository of organismal information at the genomic level, is quite susceptible to being damaged. Indeed, the loss of DNA integrity is extremely common: 10 000 DNA lesions occur per cell per day on average [1]. Preserving the integrity of information in DNA is of foremost importance due to the impact it has on processes, such as carcinogenesis, autoimmune diseases, ageing and other common pathologies [5–7]. The information content in the DNA may be damaged by a number of endogenous and exogenous

causes. The metabolism and function of the cell may produce DNA-damaging elements, such as reactive oxygen species, dehydration and other sources of ionic variations in the cell [5,6]. Environmental causes often include ionizing or UV radiation, extreme thermal variations or poisoning by chemicals known as genotoxic or mutagenic agents [1,7].

Owing to the extreme life-threatening phenomenon that DNA damage may trigger, the cells possess a *machinery* that when working properly may be able to repair the mutagenic damage caused to DNA. Such processes are generically known as the *DNA damage response* system [5,7]. The latter is composed of biochemical modules that involve DNA damage recognition; signal transduction processes leading to the activation of cellular responses to either repair DNA locally, rearrange the chromatin structure in a vast portion of DNA or, if the damage is irreparable, promote controlled mechanisms of cell death such as apoptosis [5]. DNA damage is closely related to the onset and development of cancer [2]. Genomic instability caused by mutations leads to functional genomic failure, pathway alteration and systemic disruption [8]. However, DNA damage response systems are also of importance because they are currently one focus of attention in the development of cancer therapeutics [2,9].

It is a known fact that the DNA damage phenomenon is particularly important for the development of DLBCL [10,11] in particular, since many highly susceptible genes, fragile to DNA-damaging agents, are in turn part of the DNA repair machinery [12]. For instance, in [10] the authors report that there is a molecular interaction between the MAP kinase 3 (ERK1/ERK2) complex and CHK2, a protein that plays a central role in the DNA damage checkpoint that responds to DNA double-strand breaks. *CHEK2* mutations were first reported in Li–Fraumeni familial syndrome, then the presence of damaged *CHEK2* was discovered in a number of sporadic, i.e. non-familial, malignancies and nowadays *CHEK2* is considered an important cancer susceptibility gene—though not really a tumour-suppressor gene [10]. Differences in DNA-damaged sites often lead to different gene expression patterns that have proved to be characteristic to different DLBCL molecular subtypes with different associated prognoses [13].

Understanding the physico-chemical origins of DNA damage may thus be an important research problem in relation to pathologies such as DLBCL regarding both its basic and clinical aspects. A simple model for the mechanism may be outlined as follows: certain specific regions in the genome—that may correspond to candidate hypermutation sites—possess sequence-specific features that make them more susceptible to DNA damage by ionic stress. 'If this is the case, then their corresponding denaturation/renaturation plots may show large hysteresis'. By studying the thermodynamic profiles of specific regions of the genome that are known to be hypermutated in certain pathologies (such as DLBCL), one may gain a better understanding of the mechanisms behind DNA damage and its ultimate molecular causes. The main goal of this work is, thus, to present a map of denaturation hysteresis in genes associated with DLBCL. This information may allow us to study a possible connection between DNA damage and stress-induced hysteresis.

To close the Introduction, we should point out that the novelty of this work, when compared with our recent work [3], arises from the use of a more realistic DNA model to describe the role of electrostatics on the thermodynamic properties of highly charged DNA suspensions; we have refined the Poisson–Boltzmann (PB) approach to properly account for the main features of the DNA molecule, since in [3] the DNA molecule was assumed to be a very long, almost one-dimensional, and solid cylindrical object whereas in this work we introduce a porous cylinder. Besides, we have also dealt with biological sequences for real genes (both in sequence size and composition). In particular, we here focus on the role of gene length on the hysteresis phenomenon. The rest of the manuscript is outlined as follows: §2 presents the theoretical framework of the methods and models used to study stress-induced DNA denaturation. In §3, we show the results of applying such models to DLBCL hypermutated genes, namely, *ACTB*, *MYD88*, *BTG1*, *TP53*, *KRAS*, *EZH2*, *CARD11* and *PCLO* and discuss some physico-chemical aspects in their response to ionic stress and pressure-driven denaturation that may be relevant to DNA damage. Section 4 deals with some conclusions and perspectives for future work.

2. Material and methods

2.1. Thermodynamics of stress-induced DNA denaturation

The interaction between DNA and the smaller size charged groups, also known as micro-ions, is mainly electrostatic. Its understanding is basic when phenomena, such as denaturation in charged biomolecules, are of particular interest. For instance, at low salinity, the osmotic pressure of a suspension made up of DNA molecules is determined by the electrostatic contribution to the free energy. Thus, any theory that accounts for stress-induced DNA denaturation has to include the electrostatic information during the denaturation process.

Electrostatic interactions between charged biomolecules can be well described by the PB equation [14]. In particular, we use the so-called PB-cell approximation [15]. This framework has successfully been applied to analyse the thermodynamic properties of highly charged colloids in suspension (see, for instance, [16,17] and references therein). We assume that the DNA molecule can be well-represented by a cylindrical-like structure. This is particularly motivated by the fact that experimental measurements of the micro-ion distribution around a DNA molecule agrees well with the cylindrical cell model [18]. Furthermore, this kind of approximation allows us to obtain an analytical expression of the electrostatic potential and, therefore, an analytical representation of the equation of state of DNA molecules in an aqueous-like environment [19,20]. All technical details to solve the PB-cell equation and determine the equation of state are explicitly presented in the electronic supplementary material.

Recently, we have proposed a theoretical framework that describes the process of denaturation of DNA molecules in suspension [3]. This theory makes use of an irreversible thermodynamics approach that is able to predict hysteresis curves for DNA sequences in terms of DNA configurational states, as well as system parameters like salt concentration, density and temperature [3]. Our theoretical framework provides an expression that relates the fraction of broken hydrogen bonds, ΔB_a, with the osmotic pressure, $\Delta\Pi$, and the rate of energy dissipation, $T\Gamma$ (with T and Γ being the absolute temperature and the constant (steady-state) non-equilibrium entropy production [3], respectively), during the denaturation process. In the particular case of a cylindrical-like DNA molecule, the fraction of broken hydrogen bonds reads as follows:

$$\Delta B_a = \frac{T\Gamma - ((10\,\mathrm{cm})^3/c_{\mathrm{DNA}}N_{\mathrm{A}})\Delta\Pi}{(l\,k_{\mathrm{B}}(10\,\mathrm{cm})^3/4l_{\mathrm{B}}F(T)N_{\mathrm{A}}V_{\mathrm{DNA}})\int((\chi(c_{\mathrm{DNA}})/c_{\mathrm{DNA}}^2)\mathrm{d}c_{\mathrm{DNA}})}, \tag{2.1}$$

where $F(T) \equiv dB_a/dT$ is the rate of temperature-broken hydrogen bonds, k_B is the Boltzmann's constant, l_B is Bjerrum's length, N_A is Avogadro's number, c_{DNA} is the molar concentration of DNA, $\chi(c_{DNA})$ is the normalized compressibility and $V_{DNA} = \pi a^2 l$ is the volume of a cylindrical DNA molecule of length l and radius a. The quantity $F(T)$ is a factor that is known both experimentally and from models as the one proposed by Poland & Scheraga [21] and Blake *et al*. [22]. This factor can also be obtained by the MeltSim algorithm developed and implemented by Blake *et al*. [22]. MeltSim uses as input both the sequence of DNA and the salt concentration.

As stated above, ΔB_a is a phenomenological parameter representing the fraction of broken hydrogen bonds as a function of the thermodynamic state of the system. Such phenomenology can be traced back to eqn 1 of [3]; it is introduced by means of the memory function formalism (eqn (19) therein). The memory kernel introduced there has been found to be compliant with Maxwell–Cattaneo–Vernotte (MCV)-type hyperbolic transport equations typical of extended irreversible thermodynamics. The phenomenological connection is given in terms of response coefficients, via eqn (22) of [3], which relates the changes in this term to the dynamics of uncompensated heat production (akin to entropy production in linear irreversible thermodynamics). Explicit mathematical details of the formal calculation are given in [3] (eqns (22)–(35) therein), as well as in the electronic supplementary material.

ΔB_a in DNA denaturation is thermally coupled to other dissipative processes in the system in such a way that we can relate rates of change of this quantity with changes in the thermodynamic state of the system, most notably with changes in the osmotic pressure. Indeed equation (2.1) can be derived in a straightforward manner from eqn (36) in [3]; however, the model to calculate the effects of the osmotic pressure from the PB formalism (see the electronic supplementary material) in this article has vastly been improved in comparison with the one in [3].

All quantities in equation (2.1) are expressed in CGS units to allow straightforward comparison with experimental data. From equation (2.1), one can see that the denaturation process arises by a dissipative competition between entropy production and osmotic pressure effects. In this sense, osmotic pressure dynamically stabilizes DNA via a non-equilibrium coupling.

One can consider the physical limits of equation (2.1), $\Delta B_a = 0$; the system is in a non-denaturated state, and $\Delta B_a = 1$, which implies a fully denaturated state with the two strands completely separated. The scenario $\Delta B_a = 0$ corresponds to a perfect balance between thermal dissipation and osmotic effects. $\Delta B_a = 1$ implies an (relative) absence of osmotic contributions, thus allowing free thermal denaturation. It is known that hysteresis arises because of the competing dynamics of several dissipative processes [23]. In this case, the driving force is the competition between thermal dissipation and mechanical effects of osmotic origins. The latter ones considered as a result of pure electrostatic coupling.

We should remark that equation (2.1) is the cornerstone of our theoretical formulation [3]. It is a one-parameter (energy dissipation) model based on an irreversible thermodynamics formalism. Additionally, this scheme can be easily adapted to study denaturation in any charged biomolecule in suspension.

2.2. Hysteresis curves

The detection of DNA mutations produced during the denaturation–renaturation process is vital, since it is associated with the existence of diseases such as cancer. A mutation may cause a dysfunction of a protein produced by a gene; resulting in a probable damage to the body. Given the close relationship of DNA damage with hysteresis during the denaturation process [24], a systematic study will provide evidence of conditions that favour the appearance of hysteresis. We selectively study to what extent this phenomenon occurs in highly mutated regions of the genome characterized in DLBCL. To make explicit calculations and, at the same time, keeping the discussion as general as possible, we use different gene sequences taken from the National Center for Biotechnology Information [25]. To build denaturation curves, the following features and inputs are used in our theoretical approach:

Table 1. Structural features of the B-DNA molecule [26].

parameter	symbol	value (°*A*)
radius	a	10
charge separation	l_{DNA}	1.7
linear charge density	ξ	depends on l_B
Bjerrum length in water	l_B	depends on T

(1) *The sequence of gene*. Within our formulation, sequence-depending melting or DNA denaturation by temperature is explicitly included in the factor $F(T)$; the latter depends on the length and composition of the sequence, salt concentration and temperature. It is explicitly computed using the MeltSim code [22].
(2) *Structural features of DNA*. To determine the mechanical properties of the B-DNA suspension, one needs to know the structural characteristics of the molecule. The DNA considered here, independent of the gene, presents the type B structure and possesses the features summarized in table 1.

To calculate denaturation curves, one first needs to solve the cylindrical PB-cell equation to connect the electrostatic information with the EOS. From the EOS, we straightforwardly compute the normalized compressibility (see the electronic supplementary material). This information together with the function $F(T)$ is substituted into equation (2.1) to evaluate the fraction of broken hydrogen bonds. We should recall that the DNA melting temperature dependency enters into our model via the function $F(T)$, which is calculated from a stochastic matrix approach relying on the Poland Scheraga theory of DNA denaturation [21] and implemented in the MELTSIM algorithm [22]; a widely used model for thermal denaturation.

To explicitly demonstrate how a denaturation curve exhibits hysteresis, we refer to figure 1, which displays the fraction of broken hydrogen bonds as a function of osmotic pressure. This is done particularly for the *MEF2B* gene, for which hysteresis becomes quite evident. Where $\Delta B = 0$ is the value of a completely joined DNA chain and $\Delta B = 1$ the value of a totally denaturated one. We consider the presence of hysteresis due to the fact that for different values of $T\Gamma$ denaturation curves become closer in the extremes, which could indicate a change from the original DNA thermal state so that the gene may be susceptible to damage.

Hysteresis as a non-equilibrium phenomenon is closely related to the presence of dissipative processes affecting the internal structure of molecular systems. Such dissipative processes affect the way such systems respond to environmental conditions. In the present case, the rationale is that genomic sequences that are more prone to be damaged by ionic/osmotic stresses are the ones that will exhibit hysteresis to a greater degree since the denaturation and renaturation curves are far from being the same. Let us recall that in the non-dissipative scenario, denaturation and renaturation processes will be described by a unique *equilibrium curve* describing an equilibrium phase transition.

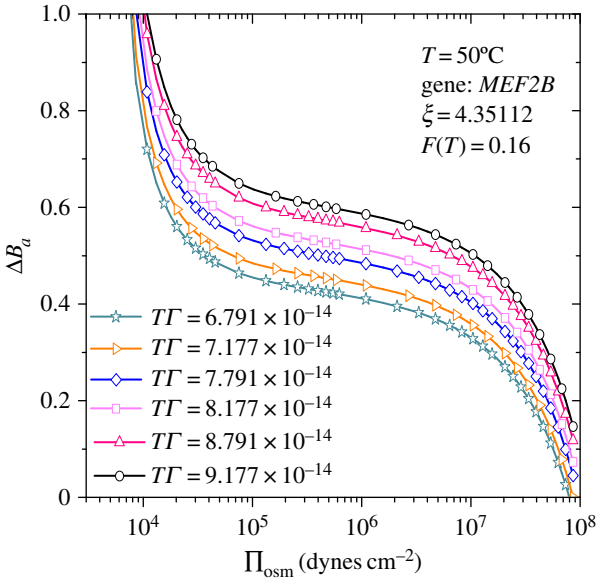

Figure 1. Example of a gene (*MEF2B*) that exhibits hysteresis in a DNA denaturation curve. The curves represent the fraction of broken hydrogen bonds as a function of the osmotic pressure. (Online version in colour.)

What we present here is evidence that genes that exhibit hysteretic behaviour are indeed more sensible to DNA damage by osmotic/ionic stress-induced mechanisms. Of course, as is often the case in biology, there are exceptions to the rule. In this case, it is not only the base composition of the given DNA that determines its *damage-ability* but as we showed, also parameters such as the length of the DNA strand.

The relationship between DNA thermal stability and the presence of mutations is not new. In the past, abnormal denaturation profiles have been linked to (and even used to detect) mutations [26,27] in a variety of settings including low-level mutations in cancer [28,29], owing to the fact that genomic instability is related to anomalous melting features. Other cases involving melting analysis to uncover mutations also invoke thermal stability considerations [30].

3. Results and discussion

3.1. Temperature-driven DNA denaturation

When talking about DNA melting in dense assemblies, one can find useful the work addressed in [31], where the importance of the (homologous *versus* random) DNA sequence is discussed explicitly. The rise of the DNA melting temperature due to electrostatic interactions predicted in such a theoretical paper has just been proved experimentally [32].

In order to characterize DNA damage in a number of genomic sequences essential for the pathogenesis of DLBCL, one first needs to calculate the composition-dependent thermal denaturation function, i.e. the rate of temperature-broken hydrogen bonds, $F(T)$, included in equation (2.1), to study the thermodynamic effects of ionic stress. For the explicit calculation of the factor $F(T)$, we explore the damage in eight genes associated with the pathogenesis of DLBCL. These genes are *ACTB*, *MYD88*, *BTG1*, *TP53*, *KRAS*, *EZH2*, *CARD11* and *PCLO*. They were chosen since they presented consistent mutations in DLBCL [4]. To calculate $F(T)$, we used the program MeltSim 1.0 [22]. This platform allows us to study the rate of temperature-broken hydrogen bonds using as input the sequence of the gene, the salt concentration (sodium molarity), the temperature increment and both the starting and the final temperatures.

The temperature dependence of the $F(T)$ for all the aforementioned genes is displayed in figure 2. The red arrows indicate the temperature values considered in the hysteresis curves shown further below. When comparing, for example, figure 2(*a*) with (*h*), one clearly appreciates the important effect that the size of the sequence has on $F(T)$; for the gene *ACTB* with 3454 bp the maximum peak is around 0.45, while the gene *PCLO* with 408 877 bp the maximum peak is 0.121. These differences indicate the strong dependence of $F(T)$ with the gene size.

Melting curves were calculated for a fixed sodium molarity $C_{Na} = 0.0005$ M, to comply with the MeltSim requirement of non-zero salt concentration. This low sodium concentration value does not modify significantly the electrostatic contribution due to the counterions. However, a higher concentration increases the osmotic pressure which provides greater stability to the configuration of the DNA molecule, requiring a higher temperature to break this configuration. Lower values for C_{Na} show spikes in the breakage of hydrogen bonds in temperatures below the cell temperature ($T = 37$°C).

3.2. Pressure-driven DNA denaturation

Physico-chemical processes, other than temperature increase, commonly trigger *in vivo* DNA melting that may potentially lead to mutation. These processes include chemical damage, radiation-enhanced melting and, of course, electrostatic interactions with the local ionic environment. The mutagenic character of chemical DNA damage and radiation has extensively been covered in the DNA biophysics literature. However, the effects of the latter has largely been neglected up to this day, with the exceptions of the studies of Cherstvy *et al.* (see, for instance, [33]) and some previous work from our group.

Abnormal DNA melting processes are known to have potential mutagenic character. Indeed, the role that DNA-destabilizing agents may have in the onset of cancer (and even in therapeutic interventions) has largely been discussed (see, for instance, [34–39]). Most of the discussion around this issue has been focused on the role that chemical denaturating agents may have in cancer-related mutagenesis. However, as a whole phenomenon, DNA melting sensitivity has been linked to cancer-related mutagenesis for many years now [40,41].

As we already stated, less attention has been paid to the potentially mutagenic effects of stress-induced DNA denaturation. This result is counterintuitive, since there is a large literature account of the role that double- and single-strand breaks in DNA may have in mutagenesis and cancer [29,35–37]. For this reason, we have decided to investigate the possible effects that osmotic pressure-enhanced DNA melting may have on specific regions in the genome (previously associated with abnormal mutation rates) linked to a quite specific common neoplasm (in this case DLBCL), whose mutational landscape has been recently studied in a multi-centric collaborative effort in which one of us participated [4].

Enhanced DNA opening may thus lead to damaged mechanisms of excision repair, not only leading to mutation but also affecting the mechanisms of DNA repair [42] with known carcinogenic effects [43–45].

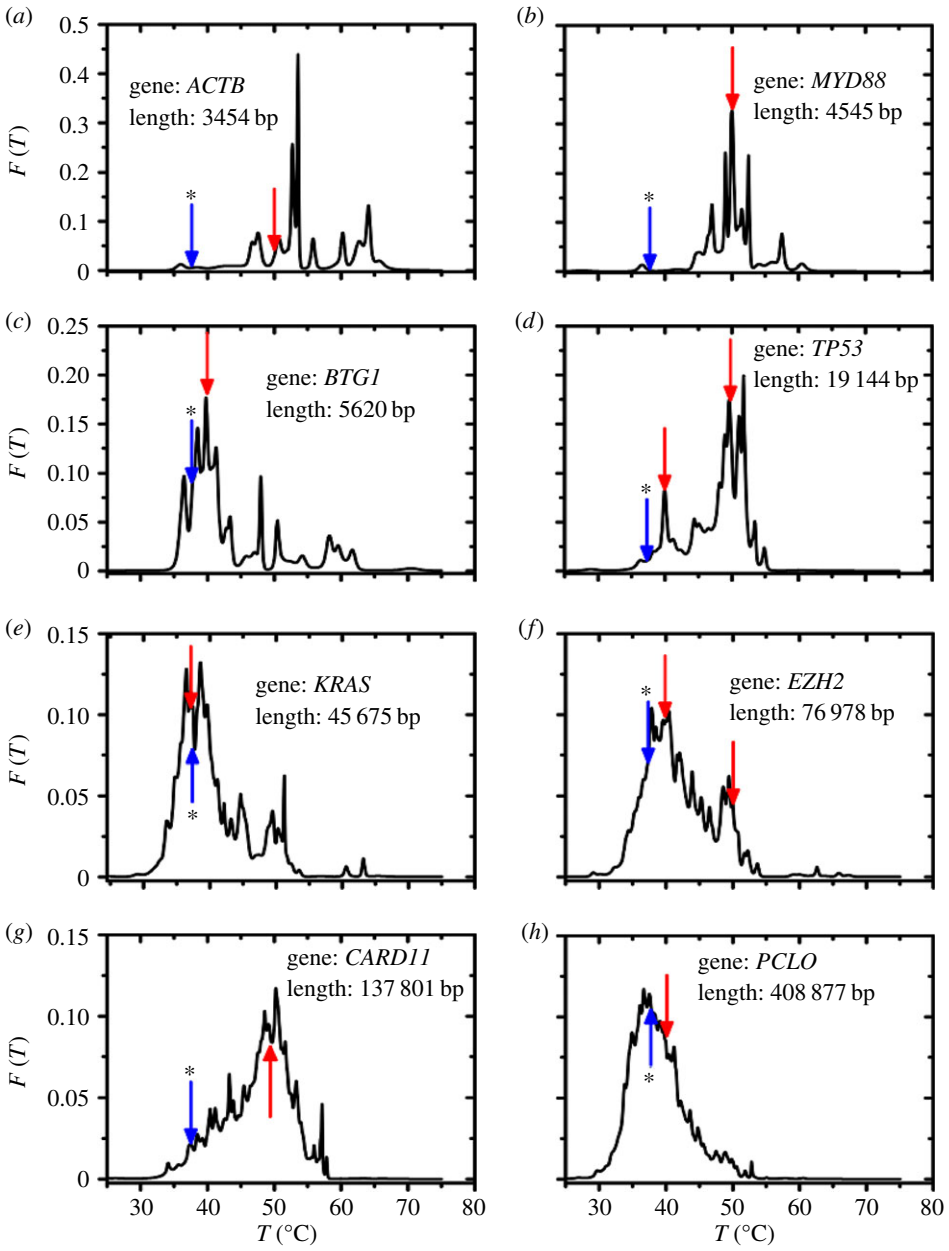

Figure 2. Rate of temperature-broken hydrogen bonds $F(T)$. The melting curves were obtained for the genes: (*a*) *ACTB*, (*b*) *MYD88*, (*c*) *BTG1*, (*d*) *TP53*, (*e*) *KRAS*, (*f*) *EZH2*, (*g*) *CARD11* and (*h*) *PCLO*. The red arrows (those with no asterisk) indicate the temperature value used in the calculation of the denaturation curves, and the blue arrows (marked with asterisk (*)) show the physiological temperature. (Online version in colour.)

The denaturation curves for the genes previously discussed are shown in figures 3–5. These curves are calculated via equation (2.1), which depends on $T\Gamma$, the energy dissipation in the process, so we plotted several curves corresponding to different values of the dissipation $T\Gamma$. A higher $T\Gamma$ implies that a lot of energy is being dissipated by the system in a fast process, hence no hysteresis effect is expected. By contrast, lower $T\Gamma$ implies a very slow process with small dissipation so no hysteresis is shown either. Therefore, $T\Gamma$ is a measure of the possibility of hysteretic behaviour in the system and consequently is indicative of dissipative processes that may induce DNA damage. To investigate the effect of the size in the profile of denaturation, we study the *CARD11* and *PCLO* genes, which have a sequence size of over 100 000 bp. For the *CARD11* gene or regulator of cell death, we show denaturation curves for the conditions already studied (figure 3*b*). The plots display a considerable rate of hydrogen bonds breaking higher than 75%, and only present a completely denaturated state for a pair value of $T\Gamma$ at $T = 50^{\circ}$C.

In order to highlight the various degrees of hysteresis present on different molecules, figures 3–5 also display values of the minimum and maximum variance in the ΔB_a values for the denaturation plots. One should recall that differences in variance may extend over several orders of magnitude, even when B_a is a normalized quantity. The bigger the difference in variance, the higher the effect of hysteresis. Major changes within a single denaturation–renaturation curve imply a higher area in between the curves. This area is thus proportional to the degree of hysteresis and is a monotonic growing function of the energy dissipation rate. Let us also recall that the dependence with the sequence size was discussed previously and accounted in the factor $F(T)$.

Denaturation curves for the *PCLO* gene are shown in figure 3*a*. The gene has 408 877 bp and is found on chromosome 7. Studies have revealed that recurrent mutations in this gene

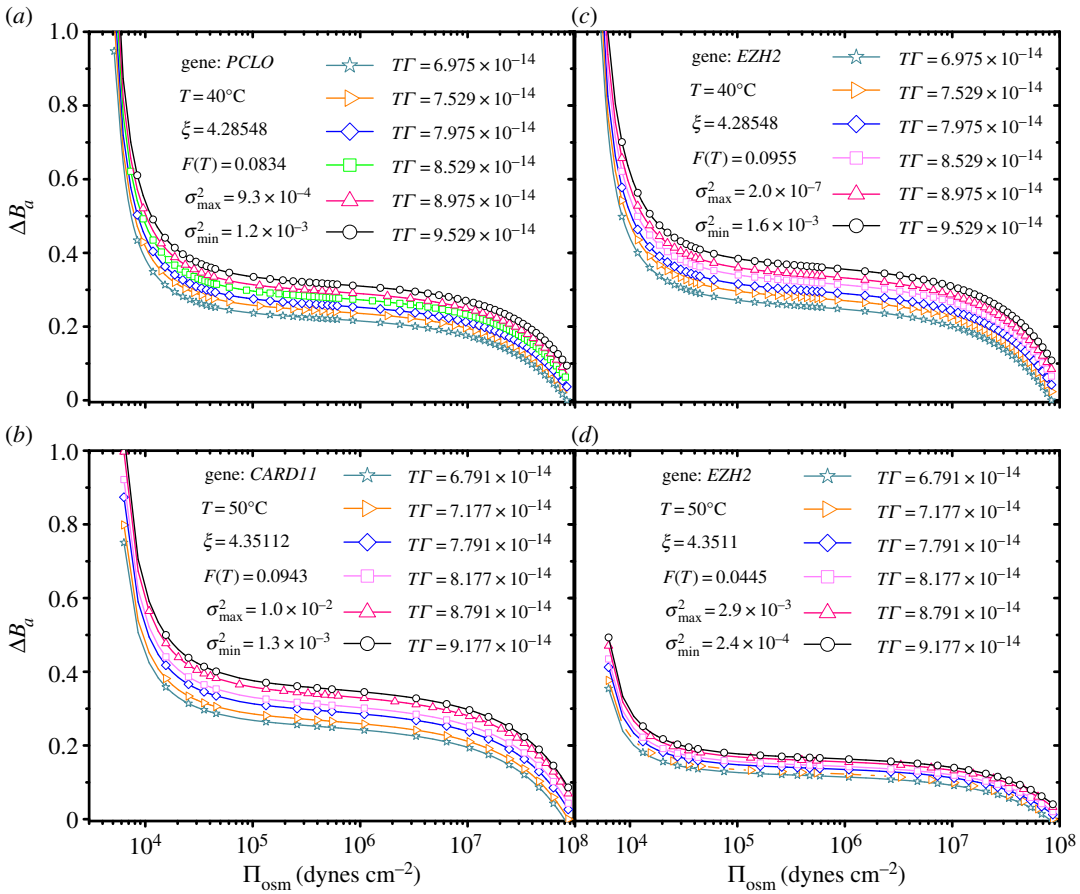

Figure 3. Denaturation curves as a function of temperature and osmotic pressure for the (*a*) *CARD11*, (*b*) *PCLO* genes and for the *EZH2* gene (*c*) $T = 40°C$, (*d*) $T = 50°C$. σ^2_{min} and σ^2_{max} denote the minimum and maximum variances, respectively. (Online version in colour.)

have been associated with cases of DLBCL [4]. The denaturation profile for this gene shows a fully denaturated state with the two strands completely separated. From figure 3, it is evident that *CARD11* exhibits hysteretic behaviour at $T = 50°C$. And the same behaviour is shown for the *PCLO* gene at $T = 40°C$. As already discussed, the hysteresis presence in this curve may be evidence of possible DNA damage under these conditions.

As we mentioned earlier, there is a potential relation with the phenomenon of stress-induced DNA damage that has been related to cellular ageing and disease effects [46]. In the particular case of the *MYD88* gene (results for this gene will be presented later), there is proof that the deficiency of this gene affects the immune system and may cause a null response of the body to produce a defence mechanism against disease [47]. Moreover, in several studies, *MYD88* has been found mutated in several patients with DLBCL [4,48]. In figure 3, we present the denaturation curves for *the human enhancer of zeste 2* or *EZH2*, a gene implicated in the progression of various types of human cancers [49]. Recurrent *EZH2* mutations have been identified in B-cell lymphomas [4]. The hysteretic behaviour at a temperature of 40°C is displayed in figure 3*c*. For this condition, DNA shows a completely denaturated state. However, when the temperature increases to $T = 50°C$ a rate of bond breaking less than 50% is exhibited.

One of the most important genes in cancer genetics is the *TP53* gene. The tumour-suppressor protein p53 is essential for regulating cell division and preventing tumour formation, reasons why it is nicknamed *guardian of the genome*. Diverse studies have demonstrated that *TP53* presents mutations in more than 50% of all types of human cancer, since it is encoded in a multifunctional protein whose absence contributes to genomic instability [50,51]. We studied the denaturation profile for *TP53* in figure 4. In the same way as in previous figures, the curves show a strong temperature dependence, which is related to the number of broken hydrogen bonds within the molecule. In both cases ((*a*) $T = 40$ and (*b*) 50°C), the gene is found in a completely denaturated state, moreover, the plots present in its extremes a closer path for the different dissipation rates enabling the identification of hysteretic behaviour for these conditions.

In figure 4, we present the denaturation map for (*c*) *BTG1*, and (*d*) *KRAS* at $T = 40°C$ and 37°C, respectively. The conditions chosen are such that the curves show complete denaturation. One can appreciate that *KRAS* presents possible damage at cell temperature, a product of the coupling between temperature and pressure in the denaturation process. *KRAS* damage is one important triggering mechanism for genomic instability. Among other things, this has led to *KRAS* being defined as an oncogene.

Finally, we show the results in figure 5 for the *ACTB* and *MYD88* genes. *ACTB* (*Actin Beta*) is located on chromosome 7. This gene provides instructions for making the protein called β-actin, which plays important roles in determining cell shape and controlling cell movement. Moreover, the mutation in this gene has been identified in some patients with DLBCL and Baraitser–Winter syndrome, a well-defined disorder characterized by distinct craniofacial features [4,52]. Even when the *ACTB* gene is found mutated in some cases,

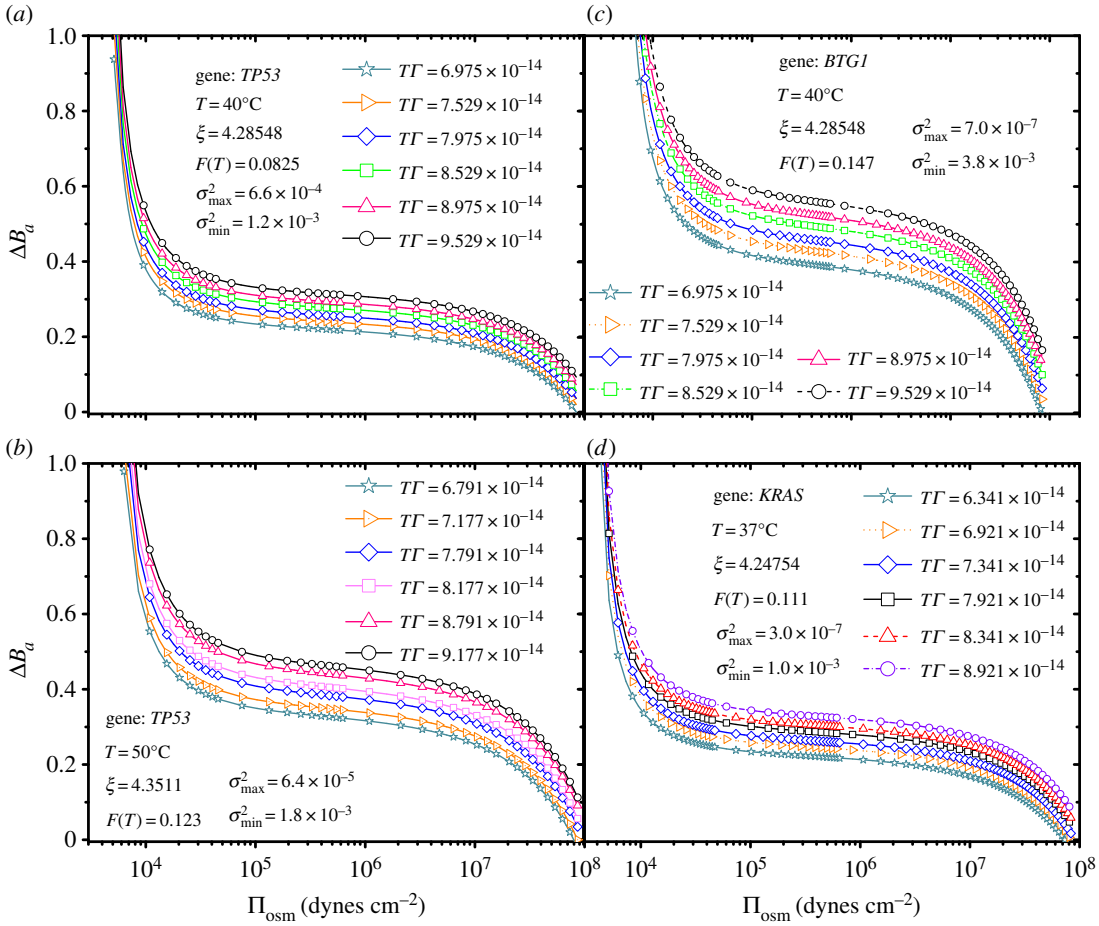

Figure 4. Denaturation curves as a function of temperature and osmotic pressure for the *TP53* gene. (*a*) $T = 40^{\circ}$C and (*b*) $T = 50^{\circ}$C. And also for the (*c*) *KRAS* and (*d*) *BTG1* genes. These curves are plotted for conditions that allow 100% of broken bonds. $\sigma^2_{\min}$ and $\sigma^2_{\max}$ denote the minimum and maximum variances, respectively. (Online version in colour.)

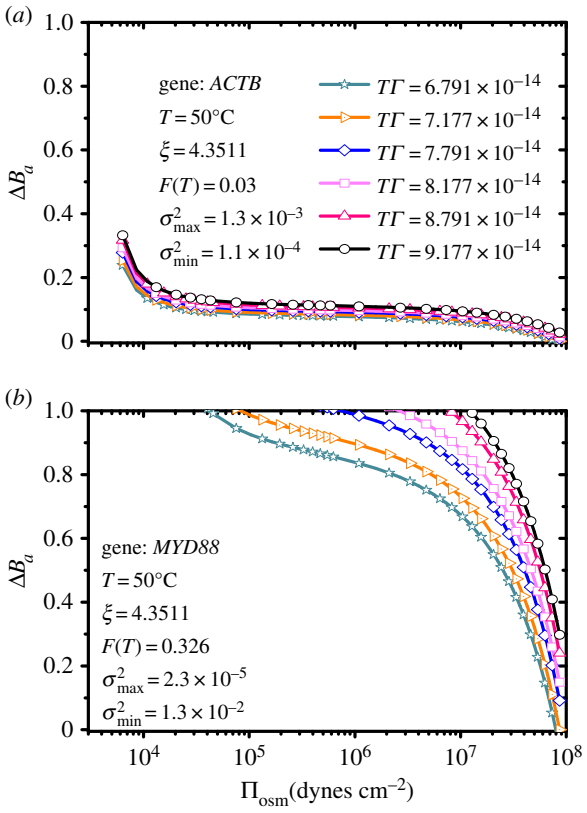

Figure 5. Denaturation curves as a function of temperature and osmotic pressure for the (*a*) *ACTB* and (*b*) *MYD88* genes. $\sigma^2_{\min}$ and $\sigma^2_{\max}$ denote the minimum and maximum variances, respectively. (Online version in colour.)

figure 5*a* does not show conclusive evidence of hysteresis in the denaturation curves, however, this does not imply that under other conditions of temperature and concentration it could not show hysteretic behaviour. By contrast, we can consider the denaturation curves given in figure 5*b* for the *myeloid differentiation primary response gene 88*, also known as *MYD88* gene. In this scenario, for the same denaturating conditions as the previous case, it is possible to observe that, under the same dissipation rate $T\Gamma$ the behaviour is distinct; we see the difference in the form of the curves, in figure 5*a* for the *ACTB* gene (for which the fully denaturated state is not present), and for the *MYD88* gene. In figure 5*b*, one sees that the denaturation occurs so rapidly that we cannot see whether there is hysteresis or not. It is important to mention that, although under these conditions neither of the *ACTB* and *MYD88* genes showed hysteresis in the denaturation curves, if we change the conditions of the system, such as the sodium concentration, the value of $F(T)$ changes and in turn, the coupling between temperature and osmotic pressure also changes giving, as a possible result, very clear hysteresis. These results are not shown here due to the fact that we are working in the no added salt regime.

4. Conclusion

In this work, we have considered hysteresis in the denaturation curve for specific genes (in particular, some genes that are known to be mutated in DLBCL) as indicative of possible

DNA damage. To measure the denaturation extent of a gene, we have used, on the one hand, a mean field theory that describes the distribution of counterions around a porous, negatively charged cylinder (the DNA model), and, on the other hand, an irreversible thermodynamics framework to measure the fraction of broken hydrogen bonds due to the coupling between the temperature and osmotic pressure. An observation of the results just presented is the important role that sequence length has on the hysteretic behaviour. The first genes displayed in the Results and discussion are the larger ones, and clearly show hysteresis in the curves. On the contrary, the last genes are the shorter ones and do not show this behaviour. In this context, the results presented for the *KRAS* gene seem to be quite significant, because the curve exhibits hysteresis even at physiological temperature, which could indicate a higher probability of DNA damage. Changes in the structure of *KRAS* have, of course, been closely related with the onset of cancer.

We also considered the denaturation of DNA sequences under no-salt conditions. Clearly, this situation does not correspond to a real physico-chemical condition, but allowed us to build, for the first time, a hysteresis map that might shed light on the possible damage that occurs in DNA. Furthermore, this case pointed towards the importance of the contribution of counterions to the phenomenon of hysteresis observed during driven-pressure DNA denaturation. The effect of salt is a topic that deserves further investigation, since such an effect might lead to a more clearly hysteretic behaviour in gene sequences.

We should point out that in this work we have implemented a more realistic DNA model (see the electronic supplementary material) and used real gene sequences. As a direct result, we emphasized the importance of sequence length on the hysteresis phenomenon. This result is similar to previous published work [31,32], where the relevance of the sequence is key when studying DNA melting.

Our results might be partially corroborated through time-consuming computer simulations using a coarse-grained model for the DNA structure. In particular, it would be rather interesting to use such a computational approach to investigate, for example, the impact on the mechanisms of hysteresis due to the B–Z DNA transition driven by salt concentration [53]. In fact, in order to reach physiological conditions, i.e. high salt concentrations, one should use a combination of computer simulations and statistical analyses to explore the thermodynamic properties of DNA melting [53,54]. Thus, more realistic models, supplemented with detailed spectroscopic [55] and calorimetric experimental data at the mesoscopic level (to date almost non-existent but foreseeable in the near future) may surely lead to a refinement of our results. In addition, incorporating other sources of chemical and physical DNA damage (for instance, oxidative stress and not only ionic stress) will be of foremost importance. All in all, there is still a lot of work to do to have a relatively complete understanding of the molecular mechanisms of DNA damage as well as its relation to oncogenic processes.

Funding statement. This work was partially supported by PIFI 3.4 - PROMEP and CONACyT (grant nos. 61418/2007, 102339/2008, and 179431/2012), as well as federal funding from the National Institute of Genomic Medicine (México). R.C-P. also acknowledges the financial support provided by the Marcos Moshinsky fellowship 2013–2014.

References

1. Seviour EG, Lin SY. 2010 The DNA damage response: balancing the scale between cancer and ageing. *Aging* **2**, 900–907.
2. Kastan MD. 2008 DNA damage responses: mechanisms and roles in human disease. *Mol. Cancer Res.* **6**, 517–524. (doi:10.1158/1541-7786.MCR-08-0020)
3. Hernández-Lemus E, Nicasio-Collazo LA, Castañeda-Priego R. 2012 Hysteresis in pressure-driven DNA denaturation. *PLoS ONE* **7** e33789. (doi:10.1371/journal.pone.0033789)
4. Lohr J *et al*. 2012 Discovery and prioritization of somatic mutations in DLBCL by whole exome sequencing. *Proc. Natl Acad. Sci. USA* **109**, 3879–3884. (doi:10.1073/pnas.1121343109)
5. Bandyopadhyay S *et al*. 2010 Rewiring of genetic networks in response to DNA damage. *Science* **330**, 1385–1389. (doi:10.1126/science.1195618)
6. Lloret J, Bolanos L, Lucas MM, Peart JM, Brewin NJ, Bonilla I, Rivilla R. 1995 Ionic stress and osmotic pressure induce different alterations in the lipopolysaccharide of a *Rhizobium meliloti* strain. *Appl. Environ. Microbiol.* **61**, 3701–3704.
7. Hara MR *et al*. 2011 A stress response pathway regulates DNA damage through β_2-adrenoreceptors and β-arrestin-1. *Nature* **477**, 349–353. (doi:10.1038/nature10368)
8. Workman CT, Mak HC, McCuine S, Tagne JB, Agarwal M, Ozier O, Begley TJ, Samson LD, Ideker T. 2006 A systems approach to mapping DNA damage response pathways. *Science* **312**, 1054–1059. (doi:10.1126/science.1122088)
9. Bensimon A, Aebersold R, Shiloh Y. 2011 Beyond ATM: the protein kinase landscape of the DNA damage response. *FEBS Lett.* **585**, 1625–1639. (doi:10.1016/j.febslet.2011.05.013)
10. Dai B *et al*. 2011 Functional and molecular interactions between ERK and CHK2 in diffuse large B-cell lymphoma. *Nat. Commun.* **2**, 402. (doi:10.1038/ncomms1404)
11. Hunt KD, Reichard KK. 2008 Diffuse large B-cell lymphoma. *Arch. Pathol. Lab. Med.* **132**, 118–124.
12. Rossi D *et al*. 2011 The host genetic background of DNA repair mechanisms is an independent predictor of survival in diffuse large B-cell lymphoma. *Blood* **117**, 2405–2413. (doi:10.1182/blood-2010-07-296244)
13. Lenz G *et al*. 2008 Molecular subtypes of diffuse large B-cell lymphoma arise by distinct genetic pathways. *Proc. Natl Acad. Sci. USA* **105**, 13 520–13 525. (doi:10.1073/pnas.0804295105)
14. Deserno M, Holm C, May S. 2000 Fraction of condensed counterions around a charged rod: comparison of Poisson–Boltzmann theory and computer simulations. *Macromolecules* **33**, 199–206. (doi:10.1021/ma990897o)
15. Alexander S, Chaikin PM, Morales GJ, Pincus P, Hone D. 1984 Charge renormalization, osmotic pressure, and bulk modulus of colloidal crystals: theory. *J. Chem. Phys.* **80**, 5776–5781. (doi:10.1063/1.446600)
16. Denton AR. 2010 Poisson–Boltzmann theory of charged colloids: limits of the cell model for salty suspensions. *J. Phys. Condens. Matt.* **22**, 364108. (doi:10.1088/0953-8984/22/36/364108)
17. Denton AR. 2012 Coarse-grained modeling of charged colloidal suspensions: from Poisson–Boltzmann theory to effective interactions. In *Electrostatics of soft and disordered matter, Proceedings of the CECAM Workshop New Challenges in Electrostatics of Soft and Disordered Matter* (eds DS Dean, J Dobnikar, A Naji, R Podgornik). Pan Stanford 2013. See http://arxiv.org/abs/1212.1758.
18. Kassapidou K, Jesse W, Kuil ME, Lapp A, Egelhaaf S, van der Maarel JRC. 1997 Structure and charge distribution in DNA and poly(styrenesulfonate) aqueous solutions. *Macromolecules* **30**, 2671–2684. (doi:10.1021/ma9617126)
19. Fuoss R, Katchalsky A, Lifson S. 1951 The potential of an infinite rod-like molecule and the distribution of the counter ions. *Proc. Natl Acad. Sci. USA* **37**, 579–589. (doi:10.1073/pnas.37.9.579)

20. Hansen L, Podgornik R, Parsegian VA. 2001 Osmotic properties of charged cylinders: critical evaluation of counterion condensation theory. *Phys. Rev. E.* **64**, 021907-4. (doi:10.1103/PhysRevE.64.021907)
21. Poland D, Scheraga HA. 1970 *Theory of helix–coil transitions in biopolymers*. New York, NY: Academic Press.
22. Blake RD, Bizzaro JW, Blake JD, Day GR, Delcourt SG, Knowles J, Marx KA, Santalucia Jr J. 1999 Statistical mechanical simulation of polymeric DNA melting with MELTSIM. *Bioinformatics* **15**, 370–375. (doi:10.1093/bioinformatics/15.5.370)
23. Hernández-Lemus E, Orgaz E. 2002 Hysteresis in nonequilibrium steady states: the role of dissipative couplings. *Rev. Mex. Fis.* **48**, 38–45.
24. Kapri R. 2012 Hysteresis and nonequilibrium work theorem for DNA unzipping. *Phys. Rev. E.* **86**, 041906. (doi:10.1103/PhysRevE.86.041906)
25. NCBI (National Center for Biotechnology Information). 2013 See http://www.ncbi.nlm.nih.gov/ (accessed: 7 October 2013).
26. Montgomery J, Wittwer CT, Palais R, Zhou L. 2007 Simultaneous mutation scanning and genotyping by high-resolution DNA melting analysis. *Nat. Protoc.* **2**, 59–66. (doi:10.1038/nprot.2007.10)
27. Zhou L, Wang L, Palais R, Pryor R, Wittwer CT. 2005 High-resolution DNA melting analysis for simultaneous mutation scanning and genotyping in solution. *Clin. Chem.* **51**, 1770–1777. (doi:10.1373/clinchem.2005.054924)
28. Oh JE, Lim HS, An CH, Jeong EG, Han JY, Lee SH, Yoo NJ. 2010 Detection of low-level *KRAS* mutations using PNA-mediated asymmetric PCR clamping and melting curve analysis with unlabeled probes. *J. Mol. Diagn.* **12**, 418–424. (doi:10.2353/jmoldx.2010.090146)
29. Pikor L, Thu K, Vucic E, Lam W. 2013 The detection and implication of genome instability in cancer. *Cancer Metastasis Rev.* **32**, 341–352. (doi:10.1007/s10555-013-9429-5)
30. Hidalgo-Grass C, Strahilevitz J. 2010 High-resolution melt curve analysis for identification of single nucleotide mutations in the quinolone resistance gene *aac(6′)-Ib-cr*. *Antimicrob. Agents Chemother.* **54**, 3509–3511. (doi:10.1128/AAC.00485-10)
31. Cherstvy AG, Kornyshev AA. 2005 DNA melting in aggregates: impeded or facilitated? *J. Phys. Chem. B* **109** 13 024–13 029. (doi:10.1021/jp051117i)
32. Sebastiani F, Pietrini A, Longo M, Comez L, Petrillo C, Sacchetti F, Paciaroni A. 2014 Melting of DNA nonoriented fibers: a wide-angle X-ray diffraction study. *J. Phys. Chem. B* **118** 3785–3792.
33. Cherstvy AG. 2011 Electrostatic interactions in biological DNA-related systems. *Phys. Chem. Chem. Phys.* **13**, 9942–9968. (doi:10.1039/c0cp02796k)
34. Kouzine F *et al*. 2013 Global regulation of promoter melting in naive lymphocytes. *Cell* **153**, 988–999. (doi:10.1016/j.cell.2013.04.033)
35. Lenglet G, David-Cordonnier MH. 2010 DNA-destabilizing agents as an alternative approach for targeting DNA: mechanisms of action and cellular consequences. *J. Nucleic Acids* **10**, 290935.
36. Dronkert MLG, Kanaar R. 2001 Repair of DNA interstrand cross-links. *Mutat. Res.* **486**, 217–247. (doi:10.1016/S0921-8777(01)00092-1)
37. Tubbs JL, Pegg AE, Tainer JA. 2007 DNA binding, nucleotide flipping, and the helix-turn-helix motif in base repair by O^6-alkylguanine-DNA alkyltransferase and its implications for cancer chemotherapy. *DNA Repair* **6**, 1100–1115. (doi:10.1016/j.dnarep.2007.03.011)
38. David-Cordonnier M-H, Laine W, Laine W. 2005 Covalent binding of antitumor benzoacronycines to double-stranded DNA induces helix opening and the formation of single-stranded DNA: unique consequences of a novel DNA-bonding mechanism. *Mol. Cancer Ther.* **4**, 71–80.
39. Stephens PJ *et al*. 2009 Complex landscapes of somatic rearrangement in human breast cancer genomes. *Nature* **462**, 1005–1010. (doi:10.1038/nature08645)
40. Kunicka JE, Olszewski W, Rosen PP, Kimmel M, Melamed MR, Darzynkiewicz Z. 1989 DNA *in situ* sensitivity to denaturation as a marker of human breast tumors. *Cancer Res.* **49**, 6347–6351.
41. Bretton PR, Darzynkiewicz Z, Henry E, Kimmel M, Fair WR, Melamed MR. 1990 DNA *in situ* sensitivity to denaturation in bladder cancer and its correlation with tumor stage. *Cancer Res.* **50**, 7912–7914.
42. Oksenych V, Coin F. 2010 The long unwinding road: XPB and XPD helicases in damaged DNA opening. *Cell Cycle* **9**, 90–96. (doi:10.4161/cc.9.1.10267)
43. Fan L, Fuss JO, Cheng QJ, Arvai AS, Hammel M, Roberts VA, Cooper PK, Tainer JA. 2008 XPD helicase structures and activities: insights into the cancer and aging phenotypes from XPD mutations. *Cell* **133**, 789–800. (doi:10.1016/j.cell.2008.04.030)
44. Helleday T, Lo J, van Gent DC, Engelward BP. 2007 DNA double-strand break repair: from mechanistic understanding to cancer treatment. *DNA Repair* **6**, 923–935. (doi:10.1016/j.dnarep.2007.02.006)
45. Hsieh P, Yamane K. 2008 DNA mismatch repair: molecular mechanism, cancer, and ageing. *Mech. Ageing Dev.* **129**, 391–407. (doi:10.1016/j.mad.2008.02.012)
46. von Zglinicki T, Burkle A, Kirkwood TB. 2001 Stress, DNA damage and ageing an integrative approach. *Exp. Gerontol.* **36**, 104962. (doi:10.1016/S0531-5565(01)00111-5)
47. von Bernuth H *et al*. 2008 Pyogenic bacterial infections in humans with MyD88 deficiency. *Science* **321**, 691–696. (doi:10.1126/science.1158298)
48. Ngo V *et al*. 2011 Oncogenically active *MYD88* mutations in human lymphoma. *Nature* **470**, 115. (doi:10.1038/nature09671)
49. Simon C *et al*. 2012 A key role for *EZH2* and associated genes in mouse and human adult T-cell acute leukemia. *Genes Dev.* **26**, 651–656. (doi:10.1101/gad.186411.111)
50. Rangel-López A, Piña-Sánchez P, Salcedo M. 2006 Variaciones genéticas del gen supresor de tumores *TP53*: relevancia y estrategias de análisis. *Rev. Invest. Cln.* **58**, 254–264.
51. Zhang X-P, Liu F, Wang W. 2012 Regulation of the DNA damage response by p53 cofactors. *Biophys J.* **102**, 2251–2260. (doi:10.1016/j.bpj.2012.04.002)
52. Rivière JB *et al*. 2012 De novo mutations in the actin genes *ACTB* and *ACTG1* cause Baraitser–Winter syndrome. *Nat. Gen.* **44**, 4. (doi:10.1038/ng.1091)
53. Cherstvy AG. 2005 Effect of DNA charge helicity on B-Z DNA transition. *J. Chem. Phys.* **123**, 116101.
54. Shin J, Cherstvy AG, Metzler R. 2014 Sensing viruses by mechanical tension of DNA in responsive hydrogels. *Phys. Rev. X* **4**, 021002.
55. Nagapriya KS, Raychaudhuri AK. 2010 Thermal fluctuation spectroscopy of DNA thermal denaturation. *Biophys. J.* **99**, 2666–2675. (doi:10.1016/j.bpj.2010.07.048)